Journal of Hazardous Materials 164 (2009) 962–967

Contents lists available at ScienceDirect

Journal of Hazardous Materials

journal homepage: www.elsevier.com/locate/jhazmat

Crystal structures, thermal decompositions and sensitivity properties of [Cu(ethylenediamine)$_2$(nitroformate)$_2$] and [Cd(ethylenediamine)$_3$](nitroformate)$_2$

Li Yang, Jin Zhang, Tonglai Zhang*, Jianguo Zhang, Yan Cui

State Key Laboratory of Explosion Science and Technology, Beijing Institute of Technology, Zhongguancun Nandajie No. 5, Haidian, Beijing 100081, PR China

ARTICLE INFO

Article history:
Received 22 May 2008
Received in revised form 28 August 2008
Accepted 29 August 2008
Available online 4 September 2008

Keywords:
Nitroformate
Complex
Crystal structure
Thermal decomposition
Sensitivity properties

ABSTRACT

Two new coordination compounds [Cu(ethylenediamine)$_2$(nitroformate)$_2$] and [Cd(ethylenediamine)$_3$](nitroformate)$_2$ were synthesized and characterized through elemental analysis, IR and UV spectra. Their crystal structures were determined through X-ray single crystal diffraction. The first compound crystallizes in the triclinic space group $P\bar{1}$; the second one crystallizes in the orthorhombic space group *Pbca*. For the first compound, central Cu(II) ion is hexa-coordinated with two ethylenediamine ligand molecules and two nitroformate anions to form the centrosymmetric octahedral structure. For the second one, central Cd(II) ion is hexa-coordinated with three ethylenediamine ligand molecules to form the slightly distorted octahedra. Through hydrogen bonds, molecules are linked together to form the three-dimensional packing diagrams. Thermal decomposition mechanisms of these two compounds were predicted through DSC, TG–DTG and FTIR analyses. In addition, the impact sensitivity, friction sensitivity and flame sensitivity were measured. All observed properties show that the first one has high energy, good thermal stability and moderate flame sensitivity.

1. Introduction

The compound trinitromethane or nitroform, that is $CH(NO_2)_3$, has been known since the end of the eighteenth century [1]. Since nitroform contains three nitro groups on the carbon atom, it was thought to be a useful explosive or explosive oxidant. However, the application of nitroform is severely constrained for its strong acidity and low decomposition temperature which is 298 K. Therefore, nitroform needs to cooperate with other compounds to form novel stable substances. Nitroformate salts have been widely studied [2–12]. For instance, hydrazinium nitroformate is a promising energetic oxidizer used to replace ammonium perchlorate in rocket propellant [13–16]. Until now, few reports about nitroformate coordination compounds have been found. Because ethylenediamine (abr. en) have strong coordination capacity, some new compounds consisting of nitroformate as anion, en as ligand and metal ion as cation may be designed as new energetic compounds.

Therefore, [Cu(ethylenediamine)$_2$(nitroformate)$_2$] (abr. [Cu(en)$_2$(NF)$_2$]) and [Cd(ethylenediamine)$_3$](nitroformate)$_2$ (abr. [Cd(en)$_3$](NF)$_2$) were synthesized and their crystal structures were determined. The thermal decomposition mechanisms of these two complexes were predicted by using DSC, TG–DTG and FTIR techniques, the kinetic parameters of their thermal decompositions were calculated, and sensitivity properties were tested.

2. Experimental

2.1. Caution

Nitroform and the two titled compounds are energetic materials and tend to explode under certain conditions. Proper protective measures (safety glasses, face shields, leather coat, ear plugs and earthening equipment and person) should be taken during the synthesis, test and measurement processes, especially when these compounds are prepared on a larger scale.

2.2. Materials and physical measurement

All the reagents used in the synthesis of [Cu(en)$_2$(NF)$_2$] and [Cd(en)$_3$](NF)$_2$ were analytical pure and without further purification.

Elemental analyses were performed on a Flash EA 1112 full-automatic microanalyser. IR spectra were conducted on a Bruker

* Corresponding author. Tel.: +86 10 68913818; fax: +86 10 68913818.
E-mail addresses: ztlbit@bit.edu.cn, ztlbit@public.bta.net.cn (T. Zhang).

0304-3894/$ – see front matter © 2008 Published by Elsevier B.V.
doi:10.1016/j.jhazmat.2008.08.096

Equinox 55 FTIR spectrophotometer. US–vis spectra were recorded on a PGENERAL TU-1810 UV-VIS spectrophotometer.

Differential scanning calorimetry (DSC) studies were conducted on a PerkinElmer Pyris 1 Differential Scanning Calorimeter with heating rates of 2, 5, 10 and 20 K/min, respectively, using dry oxygen-free nitrogen as atmosphere with a flowing rate of 20 mL/min. Thermogravimetric analyses (TGA) were operated on a PerkinElmer Pyris 1 Thermogravimetric Analyzer operating at a heating rate of 10 K/min in a flow of dry oxygen-free nitrogen at 20 mL/min.

20 mg sample was compacted into a copper cap under the pressure of 39.2 MPa, and then used to test the impact sensitivity and flame sensitivity. The impact sensitivity was determined with a Bruceton method [17] on the standard fall hammer apparatus, and the compacted sample was hit with 0.8 kg drop hammer on the apparatus. The flame sensitivity was determined on designed flame sensitivity apparatus, the compacted sample was ignited by standard black powder pellet on the apparatus. The friction sensitivity was determined by using a standard pendulum friction sensitivity apparatus. After the sample was compressed firmly between two steel poles with mirror surfaces at the pressure of 1.96 MPa, one of the steel poles was horizontally hit with a 1 kg hammer pendulum dropping from 90°.

2.3. Synthesis

Nitroform was prepared by nitrating isopropyl alcohol in 1,2-dichloroethane, using the mixed acid consisting of nitric acid (100% purity), and sulfuric acid (98% purity) as a nitrating agent.

10 mL (0.02 mol) nitroform in 1,2-dichloroethane was cooled to 273–278 K in an ice-bath. 1.46 g (0.01 mol) basic cupric carbonate or 1.72 g (0.01 mol) cadmium carbonate was added slowly into the solution while stirring strongly and carbon dioxide was released during the reaction. After the reaction mixture were stirred for an additional 60 min, the yellow cupric nitroformate solution and the yellow cadmium nitroformate solution were filtrated and reserved.

2.4 g ethylenediamine was dissolved in 5 mL deioned water and cooled in an ice-bath. The solution of copper nitroformate or cadmium nitroformate was added drop by drop into the aqueous ethylenediamine solution at 273–78 K under stirring, after dripping, the mixture was stirred for a further 1 h to complete the reaction. The precipitate was collected by filtration, washed with cold ethanol, and air-dried. The single crystals of $[Cu(en)_2(NF)_2]$ and $[Cd(en)_3](NF)_2$ which are suitable for X-ray diffraction study were grown from the filtered reaction solutions through a slow evaporation method at 277 K for 7 days. Anal. Calcd. for $C_6H_{16}CuN_{10}O_{12}$ (%): C 14.89, H 3.34, N 28.96; found (%): C 14.87; H 3.31; N 28.99. Anal. Calcd. for $C_8H_{24}CdN_{12}O_{12}$ (%): C 16.19, H 4.04, N 28.34; found (%): C 16.25; H 4.00; N 28.64. UV/vis (H_2O): λ_{max} ($\lg\varepsilon$): 350 nm (4.158) for $[Cu(en)_2(NF)_2]$; λ_{max} ($\lg\varepsilon$): 349 nm (4.158) for $[Cd(en)_3](NF)_2$. IR (KBr pellets, 4000–400 cm^{-1}, 4 cm^{-1}): νNH 3342 vs. $\nu_{as}CH_2$ 2964 s, ν_sCH_2 2855 s, δ(NH) 1607 s, $\nu_{as}NO_2$ 1528 s, ν_sNO_2 1254 vs. δCH_2 1485 m, ν_s(C–N) 893 vs. δNO_2 786 s, ν(Cu–N) 692 m, ν(Cu–O) 530 s for $[Cu(en)_2(NF)_2]$; νNH 3363 vs. $\nu_{as}CH_2$ 2941 s, ν_sCH_2 2883 s, δ(NH) 1610 s, $\nu_{as}NO_2$ 1538 s, δCH_2 1481 m, ν_sNO_2 1259 vs. ν_s(C–N) 859 vs. δNO_2 787 s, ν(Cd–N) 632 m for $[Cd(en)_3](NF)_2$.

2.4. Crystal structure determination

The crystallographic and refinement parameters in Table 1 were collected on a Rigaku MicroMax-007 diffractometer equipped with a Saturn 70CCD using confocal monochromated Mo Kα radiation (λ = 0.71073 Å) in the ω scans mode at 113 K. Empirical absorption corrections were applied using the CrystalClear program [18]. The structure was solved by direct methods and refined by full-matrix least squares techniques based on F^2 with the SHELXTL 97 program [19]. All non-hydrogen atoms were obtained from the difference Fourier map and refined with atomic anisotropic thermal parameters. The hydrogen atoms were placed geometrically and treated by a constrained refinement.

Table 1
Crystal data and refinement parameters for $[Cu(en)_2(NF)_2]$ and $[Cd(en)_3](NF)_2$

Empirical formula	$C_6H_{16}CuN_{10}O_{12}$	$C_8H_{24}CdN_{12}O_{12}$
Formula weight	483.83	592.79
Crystal system	Triclinic	Orthorhombic
Space group	$P\bar{1}$	*Pbca*
a (Å)	8.7596(2)	8.5052(2)
b (Å)	9.4854(2)	15.754(3)
c (Å)	11.8480(2)	31.783(6)
α (°)	76.35(3)	90.00
β (°)	68.37(3)	90.00
γ (°)	69.32(3)	90.00
V (Å^3)	849.8(3)	4258.6(2)
Z	2	8
D_c (g/cm^3)	1.891	1.849
Absorption coefficient (1/mm)	1.376	1.111
F(0 0 0)	494	2400
Crystal size (mm)	0.10 × 0.06 × 0.04	0.10 × 0.08 × 0.06
θ range for data collection (°)	1.86–25.02	1.28–25.02
h	$-10 \le h \le 10$	$-10 \le h \le 8$
k	$-11 \le k \le 14$	$-18 \le k \le 17$
l	$-1 \le l \le 15$	$-35 \le l \le 37$
Reflections collected	8760	23500
Independent reflections	3000 [R_{int} = 0.0201]	3750 [R_{int} = 0.0457]
Observed reflections	2582	3445
Data/restraints/parameters	3000/0/265	3750/0/298
Goodness-of-fit on F^2	1.070	1.107
Final *R* indices [$I > 2\sigma(I)$]	R_1 = 0.0266, wR_2 = 0.0646	R_1 = 0.0256, wR_2 = 0.0597
R indices (all data)	R_1 = 0.0323, wR_2 = 0.0668	R_1 = 0.0303, wR_2 = 0.0616
Largest diff. peak and hole (e/Å^3)	0.268 and −0.369	0.543 and −0.493

3. Results and discussion

3.1. Crystal structure description

The ORTEP diagrams of $[Cu(en)_2(NF)_2]$ and $[Cd(en)_3](NF)_2$ are shown in Figs. 1 and 2, respectively. Selected bond lengths and angles are listed in Tables 2 and 3, respectively. The structure analyses show that the asymmetric unit of $[Cu(en)_2(NF)_2]$ is composed of two central Cu(II) ions, four en ligand molecules and four nitroformate ligand anions while the asymmetric unit of $[Cd(en)_3](NF)_2$ is composed of one central Cd(II) ion, three en ligand molecules and two nitroformate anions.

For $[Cu(en)_2(NF)_2]$, the central Cu(II) ion is hexa-coordinated with four N atoms of four amino groups from two en ligand molecules and two O atoms of two nitro groups from two nitroformate ligand anions to form the centrosymmetric lightly distorted $[CuN_4O_2]$ octahedra. For $[Cd(en)_3](NF)_2$, the central Cd(II) ion is hexa-coordinated with six N atoms of six amino groups from three en ligand molecules to form the slightly distorted $[CdN_6]$ octahedra. The distortion of the octahedra can be demonstrated by the bond lengths and bond angles of the coordination centers.

In correspondence with the typical coordination mode, the en ligand acts as a bidentate ligand forming with the central metal ion into a disordered, five-member chelate ring. There exist two five-member chelate rings between the central Cu(II) ion and en ligands, and three for the central Cd(II) ion and en ligands. In the Cu(II) center, the dihedral angle of the two rings is 180°, resulting in a minimum steric hindrance. In the Cd(II) center, the dihedral

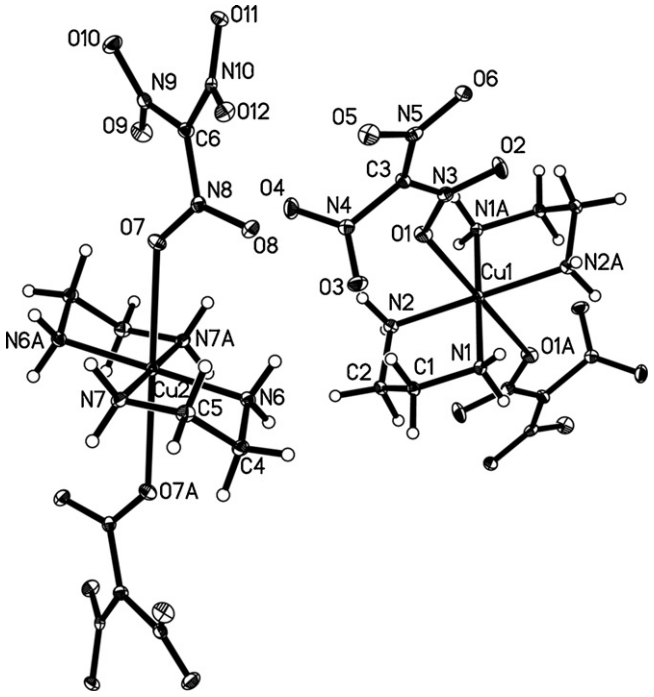

Fig. 1. ORTEP diagram (30% probability factor for thermal ellipsoid) with atomic numbering scheme for $[Cu(en)_2(NF)_2]$.

Table 2
Selected bond lengths (Å) for $[Cu(en)_2(NF)_2]$ and $[Cd(en)_3](NF)_2$[a]

$[Cu(en)_2(TNM)_2]$					
Cu1–N1#1	2.012(2)	N4–C3	1.459(3)	O9–N9	1.226(2)
Cu1–N1	2.012(2)	N5–C3	1.374(3)	O10–N9	1.236(2)
Cu1–N2#1	2.018(2)	N3–C3	1.369(3)	O7–N8	1.241(2)
Cu1–N2	2.018(2)	N1–C1	1.477(2)	O8–N8	1.237(2)
Cu1–O1	2.492(1)	N2–C2	1.483(3)	O11–N10	1.242(2)
Cu1–O1#1	2.492(1)	C1–C2	1.511(3)	O12–N10	1.237(2)
O1–N3	1.261(2)	Cu2–N6#2	2.011(2)	N8–C6	1.404(3)
O2–N3	1.232(2)	Cu2–N6	2.011(2)	N9–C6	1.423(3)
O3–N4	1.223(2)	Cu2–N7	2.019(2)	N10–C6	1.398(3)
O4–N4	1.219(2)	Cu2–N7#2	2.019(2)	N6–C4	1.478(3)
O5–N5	1.252(2)	Cu2–O7	2.517(1)	N7–C5	1.485(3)
O6–N5	1.235(2)	Cu2–O7#2	2.517(1)	C4–C5	5.140(3)
$[Cd(en)_3](TNM)_2$					
Cd1–N5	2.362(2)	O6–N9	1.248(3)	N5–C5	1.480(3)
Cd1–N1	2.365(2)	O7–N10	1.244(3)	N6–C6	1.476(3)
Cd1–N3	2.368(2)	O8–N10	1.241(3)	N7–C7	1.456(3)
Cd1–N4	2.371(2)	O9–N11	1.235(3)	N8–C7	1.373(3)
Cd1–N6	2.377(2)	O10–N11	1.244(3)	N9–C7	1.384(3)
Cd1–N2	2.384(2)	O11–N12	1.233(3)	N10–C8	1.386(3)
O1–N7	1.216(3)	O12–N12	1.234(3)	N11–C8	1.404(3)
O2–N7	1.232(3)	N1–C1	1.471(3)	N12–C8	1.422(3)
O3–N8	1.255(3)	N2–C2	1.476(3)	C1–C2	1.520(3)
O4–N8	1.236(2)	N3–C3	1.474(3)	C3–C4	1.520(4)
O5–N9	1.236(3)	N4–C4	1.469(3)	C5–C6	1.523(3)

[a] Symmetry transformations used to generate equivalent atoms: #1 $-x+2$, $-y$, $-z+1$; #2 $-x+1$, $-y+1$, $-z$.

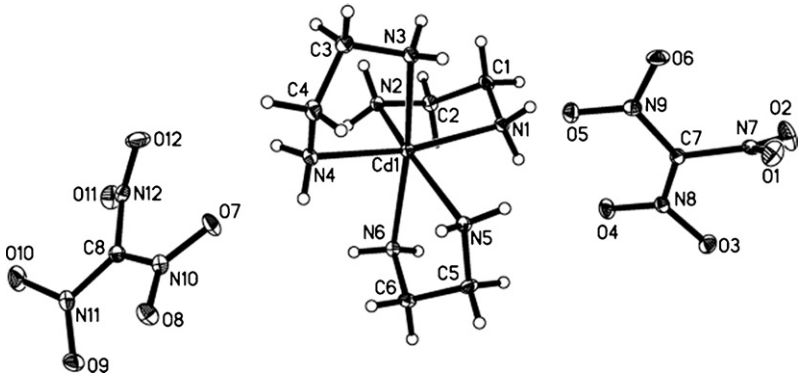

Fig. 2. ORTEP diagram (30% probability factor for thermal ellipsoid) with atomic numbering scheme for $[Cd(en)_3](NF)_2$.

Table 3
Selected bond angles (°) for $[Cu(en)_2(NF)_2]$ and $[Cd(en)_3](NF)_2$[a]

$[Cu(en)_2(TNM)_2]$					
N1#1–Cu1–N1	180.00	O6–N5–O5	123.55(2)	O7#2–Cu2–N7	88.08(1)
N1#1–Cu1–N2#1	84.36(7)	N3–C3–N5	126.76(2)	O7#2–Cu2–O7	180.00
N2#1–Cu1–N2	179.99(1)	N3–C3–N4	115.90(2)	O8–N8–O7	122.38(2)
O1–Cu1–N1#1	84.24(1)	N5–C3–N4	116.35(2)	O9–N9–O10	123.19(2)
O1#1–Cu1–N2	81.90(1)	N6#2–Cu2–N6	179.99(2)	O12–N10–O11	121.98(2)
O1#1–Cu1–O2	180.00	N6#2–Cu2–N7#2	84.90(8)	N10–C6–N8	120.10(2)
O2–N3–O1	122.78(2)	N7–Cu2–N7#2	180.00	N10–C6–N9	119.29(2)
O4–N4–O3	124.01(2)	O7–Cu2–N6#2	80.53(1)	N8–C6–N9	120.40(2)
$[Cd(en)_3](TNM)_2$					
N5–Cd1–N1	90.45(7)	N4–Cd1–N6	94.42(7)	O8–N10–O7	121.80(2)
N5–Cd1–N3	98.39(7)	N5–Cd1–N2	158.07(7)	O9–N11–O10	122.80(2)
N1–Cd1–N3	93.10(7)	N1–Cd1–N2	75.56(7)	O11–N12–O12	122.80(2)
N5–Cd1–N4	91.96(7)	N3–Cd1–N2	99.14(7)	N8–C7–N9	125.70(2)
N1–Cd1–N4	168.42(7)	N4–Cd1–N2	105.15(7)	N8–C7–N7	116.40(2)
N3–Cd1–N4	75.34(7)	N6–Cd1–N2	88.76(7)	N9–C7–N7	117.07(2)
N5–Cd1–N6	76.12(7)	O1–N7–O2	124.60(2)	N10–C8–N11	122.30(2)
N1–Cd1–N6	97.15(7)	O4–N8–O3	121.90(2)	N10–C8–N12	119.90(2)
N3–Cd1–N6	168.37(7)	O5–N9–O6	122.80(2)	N11–C8–N12	117.80(2)

[a] Symmetry transformations used to generate equivalent atoms: #1 $-x+2$, $-y$, $-z+1$; #2 $-x+1$, $-y+1$, $-z$.

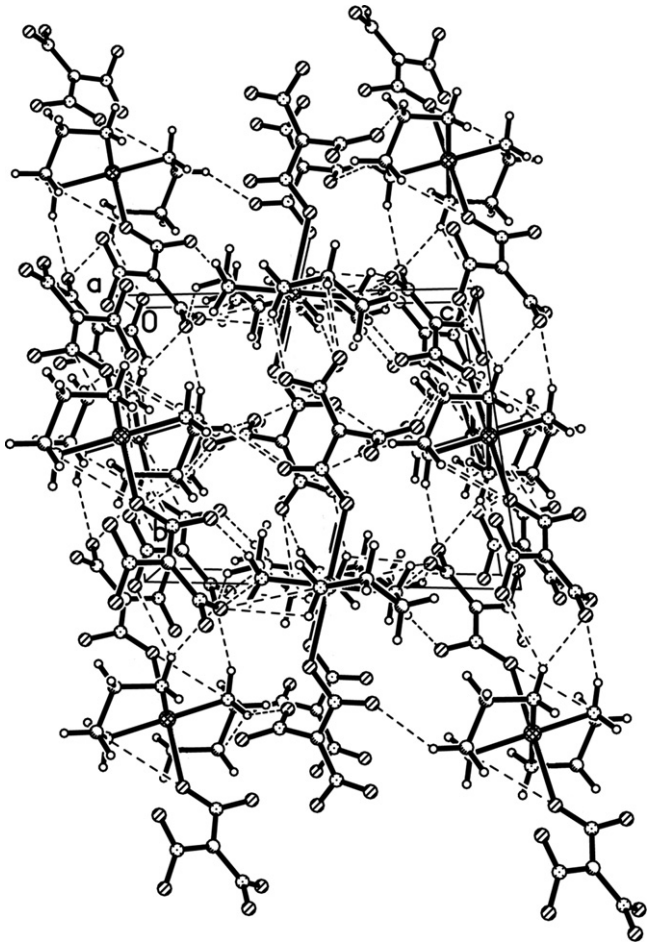

Fig. 3. The three-dimensional packing diagram of $[Cu(en)_2(NF)_2]$ viewed along the *a* axis.

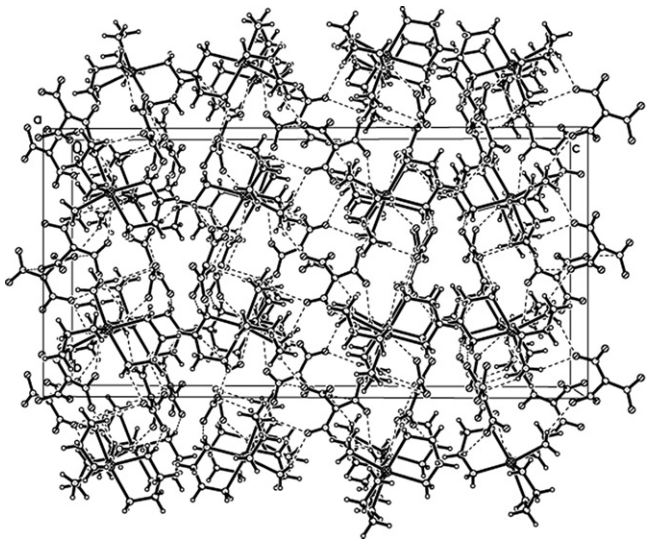

Fig. 4. The three-dimensional packing diagram of $[Cd(en)_3](NF)_2$ viewed along the *a* axis.

Table 4
Hydrogen bond distances and angles for $[Cu(en)_2(NF)_2]$[a]

D–H···A	d(D–H) (Å)	d(H···A) (Å)	d(D···A) (Å)	D–H···A (°)
N1–H1A···O6#1	0.920	2.310	3.124(2)	147.00
N1–H1B···O5#2	0.920	2.300	3.077(3)	143.00
N2–H2B···O8#3	0.920	2.270	3.156(3)	163.00
N6–H6A···O11#1	0.920	2.260	3.130(2)	157.00
N6–H6B···O3	0.920	2.500	3.244(3)	139.00
N7–H7A···O10#4	0.920	2.520	3.238(3)	135.00
N7–H7A···O11#4	0.920	2.260	3.112(2)	154.00
N7–H7B···O4#5	0.920	2.590	3.487(3)	165.00
C1–H1D···O5#1	0.990	2.550	3.322(3)	135.00
C5–H5A···O4#6	0.990	2.530	3.283(3)	133.00
C5–H5A···O9#6	0.990	2.530	3.318(3)	136.00

[a] Symmetry transformations used to generate equivalent atoms: #1, $x, y-1, z$; #2 $-x+1, -y+1, -z+1$; #3 $x+1, y-1, z$; #4 $-x+1, -y+2, -z$; #5 $-x+1, -y+1, -z$; #6 $x-1, y, z$.

angles between the rings are almost 90°, leading to the least steric hindrance and the stable space structure.

Nitroformate anions in the two title complexes have both the characteristic C–N_3 plane and the typical conformation of the nitro groups, which have been previously described in the literatures [5,7–12]. There exist two conformations of nitroformate anions in the Cu(II) center and the Cd(II) center, respectively. One is that two of the nitro groups are almost coplanar with the C–N_3 plane, whereas the third one is twist out of plane at a certain angle. The other is that nitro groups of nitroformate anions adopt a propeller-like structure twisted more evenly compared with the C–N_3 plane. For $[Cu(en)_2(NF)_2]$, the dihedral angles between the nitro groups and the C–N_3 planes are 9.4° (N3, Fig. 1), 99.2° (N4, Fig. 1), 2.1° (N5, Fig. 1), 23.1° (N8, Fig. 1), 24.2° (N9, Fig. 1) and 24.2° (N10, Fig. 1). For $[Cd(en)_3](NF)_2$, the dihedral angles between the nitro groups and the C–N_3 planes are 61.9° (N7, Fig. 2), 8.0° (N8, Fig. 2), 6.1° (N9, Fig. 2), 12.5° (N10, Fig. 2), 25.9° (N11, Fig. 2) and 33.6° (N12, Fig. 2). Because the nitroformate anions in $[Cu(en)_2(TNM)_2]$ take part in coordination but ones in $[Cd(en)_3](NF)_2$ are only counter anions and don't take part in coordination, $[Cu(en)_2(TNM)_2]$ has high energy, low thermal stability and high sensitivity, which can be confirmed by thermal decomposition and sensitivity experiments.

As shown in Figs. 3 and 4, there are intramolecular and intermolecular hydrogen bonds in the two title compounds to link the molecules into a three-dimensional network structure. The hydrogen bond distances and angles are summarized in Tables 4 and 5. For $[Cu(en)_2(NF)_2]$, all the oxygen atoms of nitro groups in the anions, except O1, O2, O7 and O12, act as acceptors in hydrogen bonds to the nitrogen and carbon atoms of en ligands with distances of 3.077–3.487 Å and angles of 133–165°. For $[Cd(en)_3](NF)_2$, all the oxygen atoms of nitro groups in the anions, except O1 and O11, act as acceptors in hydrogen bonds to the nitrogen and carbon atoms of en ligands with distances of 3.030–3.300 Å and angles of 130.40–161.30°. These extensive hydrogen bonds also make an

Table 5
Hydrogen bond distances and angles for [Cd(en)3](NF)2[a]

D–H···A	d(D–H) (Å)	d(H···A) (Å)	d(D···A) (Å)	D–H···A (°)
N1–H1A···O2#1	0.900	2.440	3.216(3)	144.40
N5–H5B···O12#2	0.900	2.310	3.084(3)	144.10
N3–H3A···O8#3	0.900	2.360	3.070(3)	136.30
N3–H3A···O9#3	0.900	2.590	3.300(3)	136.70
N1–H1B···O3#4	0.900	2.230	3.043(3)	150.30
N6–H6B···O3#4	0.900	2.240	3.047(3)	149.50
N2–H2A···O6#5	0.900	2.550	3.203(3)	130.40
N2–H2B···O10#6	0.900	2.250	3.056(3)	149.40
N4–H4A···O7#7	0.900	2.160	3.030(3)	161.30
N6–H6A···O8#7	0.900	2.420	3.236(3)	151.40
N5–H5A···O5	0.900	2.370	3.161(3)	146.60
N5–H5A···O4	0.900	2.380	3.095(3)	136.70

[a] Symmetry transformations used to generate equivalent atoms: #1 $-x+1, -y+1, -z$; #2 $x+1/2, y, -z+1/2$; #3 $-x+1, y+1/2, -z+1/2$; #4 $x-1/2, -y+1/2, -z$; #5 $-x+1/2, y-1/2, z$; #6 $-x, y+1/2, -z+1/2$; #7 $x-1/2, y, -z+1/2$.

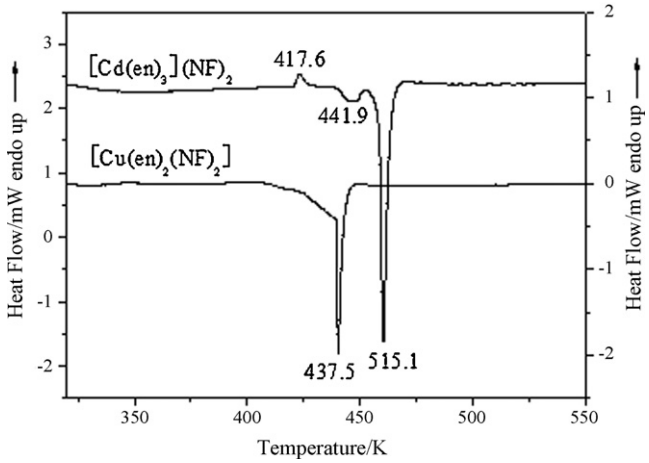

Fig. 5. DSC curves of $[Cu(en)_2(NF)_2]$ and $[Cd(en)_3](NF)_2$ at a heating rate of 10 K/min.

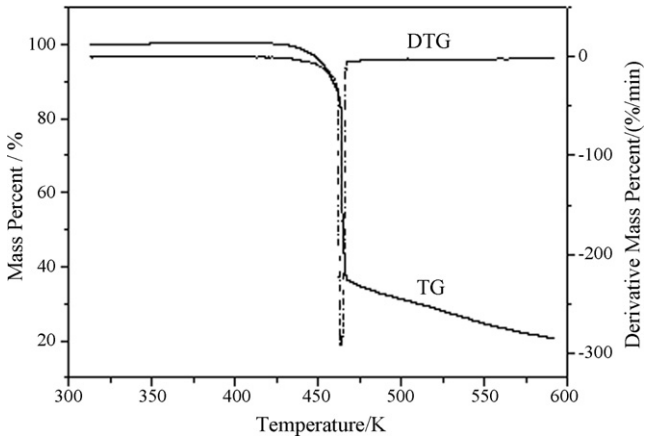

Fig. 7. TG–DTG curves of $[Cd(en)_3](NF)_2$ at a heating rate of 10 K/min.

important contribution to the stability of the two title coordination compounds.

3.2. Thermal decomposition mechanism

Under the linear heating rate of 10 K/min, the DSC and TG–DTG experiments were carried out in order to investigate the thermal decomposition characters of $[Cu(en)_2(NF)_2]$ and $[Cd(en)_3](NF)_2$ (Figs. 5–7). In the DSC curves, the two compounds behave different heat effects. For $[Cu(en)_2(NF)_2]$, there is a single sharp exothermic peak with onset temperature at 419 K and peak temperature at 437.5 K. The exothermic enthalpy change is 50.47 kJ/mol. Corresponding to this exothermic process, a very fast mass loss process appears in the range of 404–440 K in the TG curve with the whole mass loss of 83.98%. It corresponds to the largest mass loss rate of 779.11 %/min at 427.3 K in the DTG curve. $[Cu(en)_2(NF)_2]$ decomposes completely during this process. The final residue might be CuO (found 16.02%, cal. 16.44%). In the infrared spectrum of the final decomposed residue at 500 K, the disappearance of the characteristic absorption bands of $[Cu(en)_2(NF)_2]$ and the existence of the absorption peaks around 582 and 516 cm^{-1} also prove the final decomposed residue is CuO [20].

For $[Cd(en)_3](NF)_2$, one endothermic process is followed by one weak and one intense exothermic process. The initial endothermic process is at 413–422 K with the peak temperature at 417.6 K. The endothermic enthalpy change is 46.8 kJ/mol. The TG–DTG curves (Fig. 7) indicate that there is no mass loss in this temperature range.

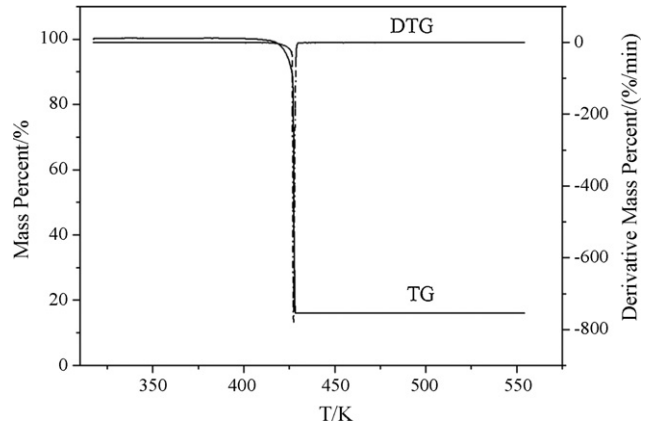

Fig. 6. TG–DTG curves of $[Cu(en)_2(NF)_2]$ at a heating rate of 10 K/min.

The infrared spectra of $[Cd(en)_3](NF)_2$ at room temperature and the solid residue at 425 K have no big differences. These prove that the first peak of the DSC curve only is the melting endothermic peak. Following this endothermic process, there are two intense exothermic peaks in the DSC curve with the onset temperature at 435 K and the peak temperatures at 443 and 465 K. The total exothermic enthalpy of two processes is 534.4 kJ/mol. Corresponding to the two exothermic processes, there is a prominent mass loss of 64% in the TG curve, and the maximum rate of mass loss of 291.10 %/min is observed at 463 K. $[Cd(en)_3](NF)_2$ decomposes completely during these processes. The last residue of the thermal decomposition process is 20.9%, which is accordant with the 21.6% value calculated for CdO. The infrared spectrum of the final decomposition residue at 500 K corresponds with the standard infrared spectrum of CdO [20], so it also proves that the final residue is CdO.

Based on the experimental and calculated results, the thermal decomposition processes of $[Cu(en)_2(NF)_2]$ and $[Cd(en)_3](NF)_2$ are proposed as follows:

$$[Cu(en)_2(NF)_2] \overset{400500\,K}{\longrightarrow} CuO + \text{gas products}$$

$$[Cd(en)_2(NF)_2] \overset{400500\,K}{\longrightarrow} CdO + \text{gas products}$$

3.3. Non-isothermal kinetics analysis

Kissinger's [21] and Ozawa–Doyle's method [22,23] were applied to study the kinetics parameters based on the first exothermic peak temperatures measured from DSC curves with four different heating rates. The apparent activation energy E_K and E_O, pre-exponential factor A_K, and linear correlation coefficient R_K and R_O were shown in Table 6 (subscripts K and O denoted calculation results by Kissinger's method and Ozawa–Doyle's method, respectively).

The calculated results using both methods are within the normal range of the kinetic parameters of such thermal decomposition reaction [24], and correspond well with each other. Therefore, the Arrhenius equations of the first exothermic processes of $[Cu(en)_2(NF)_2]$ (Eq. (1)) and $[Cd(en)_3](NF)_2$ (Eq. (2)) can be expressed in E_K and $\ln A_K$ as follows:

$$\ln k = 25.39 - \frac{245.3 \times 10^3}{RT} \quad (1)$$

$$\ln k = 30.47 - \frac{270.7 \times 10^3}{RT} \quad (2)$$

Table 6
The calculated kinetic parameters for the first exothermic decomposition processes of $[Cu(en)_2(NF)_2]$ and $[Cd(en)_3](NF)_2$

β (K/min)	T_p[a] (K)	E_K[b] (kJ/mol)	R_K[b]	$\ln A_K$[b]	E_O[c] (kJ/mol)	R_O[c]
$[Cu(en)_2(NF)_2]$						
2	429.48	245.3	0.9972	25.39	239.4	0.9973
5	435.51					
10	439.54					
20	442.97					
$[Cd(en)_3](NF)_2$						
2	432.14	270.7	0.9977	30.47	264.6	0.9978
5	437.87					
10	441.92					
20	445.25					

[a] T_p: maximum peak temperature.
[b] Subscript K: Kissinger's method.
[c] Subscript O: Ozawa–Doyle's method.

These equations can be used to estimate the rate constants for the thermal decomposition processes of $[Cu(en)_2(NF)_2]$ and $[Cd(en)_3](NF)_2$, and predict their thermal decomposition mechanisms.

3.4. Sensitivity properties

In order to study the stability and the hazard, the sensitivity data of $[Cu(en)_2(NF)_2]$ and $[Cd(en)_3](NF)_2$ were measured. The test results of impact sensitivity showed that the two titled compounds did not fire at the highest apparatus limitation of 53 cm. According to the standard method [25], flame sensitivity was evaluated with the height for 50% probability of explosion ($h_{50\%}$) of the sample. The 50% firing height of $[Cu(en)_2(NF)_2]$ is calculated as 34.42 cm, and that of $[Cd(en)_3](NF)_2$ is calculated as 15.90 cm. The statistical firing rate about friction sensitivities of $[Cu(en)_2(NF)_2]$ and $[Cd(en)_3](NF)_2$ is 0%. These two titled compounds are both insensitive to mechanical stimuli and sensitive to flame at the test conditions. The flame sensitivities of the two complexes are related with their molecular structures and thermal stabilities.

4. Conclusion

The two complexes $[Cu(en)_2(NF)_2]$ and $[Cd(en)_3](NF)_2$ were prepared and characterized. In the two compounds, central metal ions, en ligand molecules and nitroformate anions are constructed to a complicated three-dimensional netted structure through coordination bonds, electrostatic forces and considerable strong hydrogen bonds. These structure characteristics of two compounds implies the good thermal stability and high sensitivity of $[Cu(en)_2(NF)_2]$, which can be confirmed by the DSC, TGA analyses and sensitivity tests. The tests obtained during this work show that $[Cu(en)_2(NF)_2]$ can be further studied for its application in the ammunition field.

Acknowledgements

The authors give thanks to the National Natural Science Foundation of China (No. 20471008) for financial supports.

Appendix A. Supplementary materials

CCDC 673636 and CCDC 686723 contain the supplementary crystallographic data for this paper. These data can be obtained free of charge via www.ccdc.cam.ac.uk/conts/retrieving.html (or from the Cambridge Crystallographic Data Centre, 12 Union Road, Cambridge CB2 1EZ, UK. Fax: +44 1223 336033).

References

[1] E. Schmidt, Constitution of tetranitromethane, Berichte 52B (1919) 400–404.
[2] N.I. Golovina, L.O. Atovmyan, X-ray structure study of potassium nitroform, Zh. Strukt. Khim. 8 (1967) 307–311.
[3] N.V. Grigor'eva, N.V. Margolis, I.N. Shokhor, X-ray diffraction study of the structure of trinitromethane salts, Zh. Strukt. Khim. 7 (1966) 278–280.
[4] N.V. Grigor'eva, N.V. Margolis, I.N. Shokhor, Anions of dinitromethyl compounds. VIII. Refinement of the structures of the rubidium salts of trinitromethane and dinitroacetonitrile, Zh. Strukt. Khim. 9 (1968) 550–552.
[5] M.J. Brookes, N.J. Jonathan, Structure of trinitromethane and its covalent mercury salt, Chem. Soc. 9 (1968) 2266–2269.
[6] M. Krishnan, P. Sjoberg, P. Politzer, Guanidinium trinitromethanide, J. Chem. Soc. 9 (1989) 1237–1242.
[7] H.L. Ammon, C.S. Choi, A. Bashir-Hashemi, Structure of 1-adamantanylammonium trinitromethide, Acta Cryst. C C45 (1989) 319–321.
[8] H.L. Ammon, C.S. Choi, A. Bashir-Hashemi, Structure of 1,4-cubanediyldiammonium bis(trinitromethanide), Acta Cryst. C C46 (1990) 295–298.
[9] J.C. Bryan, M.N. Burnett, A.A. Gakh, Tetrabutylammonium and cesium salts of trinitromethane, Acta Cryst. C C54 (1998) 1229–1233.
[10] M. Göbel, T.M. Klapötke, P. Mayer, Crystal structures of the potassium and silver salts of nitroform, Z. Anorg. Allg. Chem. 632 (2006) 1043–1050.
[11] M. Göbel, T.M. Klapötke, Potassium-, ammonium-, hydrazinium-, guanidinium-, aminoganidinium-, diaminoguanidinium-, triaminoguanidinium- and melaminiumnitroformate—synthesis, characterization and energetic properties, Z. Anorg. Allg. Chem. 633 (2007) 1006–1017.
[12] Y.E. Huang, H.X. Gao, B. Twamley, J.M. Shreeve, Synthesis and characterization of new energetic nitroformate salts, Eur. J. Inorg. Chem. 14 (2007) 2025–2030.
[13] H.F.R. Schöyer, W.H.M. Welland-Veltmans, J. Louwers, Overview of the development of hydrazinium nitroform, J. Propul. Power 18 (2002) 131–137.
[14] H.F.R. Schöyer, W.H.M. Welland-Veltmans, J. Louwers, Overview of the development of hydrazinium nitroform based solid propellants, J. Propul. Power 18 (2002) 138–145.
[15] G.K. Willians, T.B. Brill, Thermal decomposition of energetic material 67. Hydrazinium nitroformate (HNF) rates and pathways under combustionlike conditions, Combust. Flame 102 (1995) 418–426.
[16] M.A. Bohn, Thermal stability of hydrazinium nitroformate (HNF) assessed by heat generation rate and heat generation and mass loss, J. Pyrol. 26 (2007) 65–94.
[17] W.J. Dixon, A.M. Mood, A method for obtaining and analyzing sensitivity data, J. Am. Stat. Assoc. 43 (1948) 109–126.
[18] CrystalClear Software 1.3.6, Rigaku Corporation, Rigaku/MSC 2005, 9009 New Trails Dr., The Woodlands, TX, USA.
[19] G.M. Sheldrick, SHELXTL-97: Structure Determination Software Programs, Bruker Analytical of X-ray System, Inc., Madison, WI, USA, 1997.
[20] R.A. Nyquist, R.O. Kagel, Infrared Spectra of Inorganic Compounds, Academic Press, New York, 1971.
[21] H.E. Kissinger, Reaction kinetics in differential thermal analysis, Anal. Chem. 29 (1957) 1702.
[22] T. Ozawa, A new method of analyzing thermo-gravimetric data, Bull. Chem. Soc. Jpn. 38 (1965) 1881.
[23] C.D.J. Doyle, Kinetic analysis of thermo-gravimetric data, J. Appl. Polym. Sci. 5 (1961) 285.
[24] R.Z. Hu, A.Q. Yang, Y.J. Ling, The determination of the most probable mechanism function and three kinetic parameters of exothermic decomposition reaction of energetic materials, Thermochim. Acta 123 (1988) 135.
[25] Z.T. Liu, Y.L. Lao, Initiating Explosive Experimental, Beijing Institute of Technology, China, 1995.